



Providing Choice & Value
Generic CT and MRI Contrast Agents

**FRESENIUS
KABI**

CONTACT REP

AJNR

This information is current as
of July 30, 2025.

Estimating Flow Direction of Circle of Willis Using Dynamic Arterial Spin Labeling Magnetic Resonance Angiography

Kaiyu Zhang, Halit Akcicek, Gen Shi, Gador Canton, Josh Liu,
Yin Guo, Xin Wang, Li Chen, Kristi D. Pimentel, Ebru Yaman
Akcicek, Xihe Tang, Yongjian Jin, Xuesong Li, Niranjan Balu,
Thomas S. Hatsukami, Mahmud Mossa-Basha, Zhensen Chen
and Chun Yuan

AJNR Am J Neuroradiol published online 24 May 2024
<http://www.ajnr.org/content/early/2024/05/24/ajnr.A8355>

Estimating Flow Direction of Circle of Willis Using Dynamic Arterial Spin Labeling Magnetic Resonance Angiography

Kaiyu Zhang, Halit Akcicek, Gen Shi, Gador Canton, Josh Liu, Yin Guo, Xin Wang, Li Chen, Kristi D. Pimentel, Ebru Yaman Akcicek, Xihe Tang, Yongjian Jin, Xuesong Li, Niranjana Balu, Thomas S. Hatsukami, Mahmud Mossa-Basha, Zhensen Chen, and Chun Yuan

ABSTRACT

BACKGROUND AND PURPOSE: The Circle of Willis (COW) is a crucial mechanism for cerebral collateral circulation. This proof-of-concept study aims to develop and assess an analysis method to characterize the hemodynamics of the arterial segments in COW using arterial spin labeling (ASL) based non-contrast enhanced dynamic magnetic resonance angiography (dMRA).

MATERIALS AND METHODS: The developed analysis method uses a graph model, bootstrap strategy, and ensemble learning methodologies to determine the time-curve shift from ASL dMRA to estimate the flow direction within the COW. The performance of the method was assessed on 52 subjects, using the flow direction, either antegrade or retrograde, derived from 3D phase contrast (PC) MRI as the reference.

RESULTS: A total of 340 arterial segments in COW were evaluated, among which 30 (8.8%) had retrograde flow according to 3D PC. The ASL dMRA-based flow direction estimation has an accuracy, sensitivity, and specificity of 95.47%, 80%, and 96.34%, respectively.

CONCLUSIONS: Using ASL dMRA and the developed image analysis method to estimate the flow direction in COW is feasible. This study provides a new method to assess the hemodynamics of the COW, which could be useful for the diagnosis and study of cerebrovascular diseases.

ABBREVIATIONS: COW = Circle of Willis; ASL = arterial spin labeling; dMRA = dynamic magnetic resonance angiography; PC = phase contrast.

Received month day, year; accepted after revision month day, year.

From the Department of Bioengineering (K.Z., J.L., Y.G., C.Y.), Department of Radiology (G.C., K.D.P., N.B., M.M., C.Y.), Department of Electrical and Computer Engineering (X.W., L.C.), and Department of Surgery (T.S.H.), University of Washington, Seattle, Washington, USA; Department of Radiology and Imaging Sciences, University of Utah (H.A., E.Y.A., C.Y.); School of Engineering Medicine and School of Biological Science and Medical Engineering (G.S.), Beihang University, Beijing, China; Department of Neurosurgery (X.T., Y.J.), Aviation General Hospital of China Medical University, Beijing, China; School of Computer Science and Technology (X.L.), Beijing Institute of Technology, Beijing, China; Key Laboratory of Computational Neuroscience and Brain-Inspired Intelligence (Z.C.), Ministry of Education, Beijing, China; Institute of Science and Technology for Brain-Inspired Intelligence (Z.C.), Fudan University, Shanghai, China.

Disclosure of potential conflicts of interest should be included here.

Please address correspondence to Zhensen Chen, Ph.D., Institute of Science and Technology for Brain-Inspired Intelligence, Fudan University, Shanghai, China, 200433; e-mail: zhensench@fudan.edu.cn.

SUMMARY SECTION

PREVIOUS LITERATURE: Circle of Willis (COW) is an important component of cerebral collateral circulation. The arterial structure of COW and its clinical relevance have been extensively studied using traditional angiographic techniques such as DSA, CTA, and MRA. However, the flow in COW is less studied partially due to the limitations of the existing techniques. ASL dynamic MRA is an emerging non-contrast enhanced technique that can provide both structural and flow information of intracranial arteries. However, its capability for estimating the flow direction in COW arteries is underexplored and the corresponding post-processing method is yet to be developed.

KEY FINDINGS: A novel post-processing method to determine the blood flow direction of the COW arteries from the ASL dMRA was developed, with the accuracy rate, sensitivity, and specificity being 95.47%, 80%, and 96.34%, respectively. Retrograde flow, occurring in 8.8% of the evaluated arterial segments, were successfully detected.

KNOWLEDGE ADVANCEMENT: This study demonstrated that ASL dMRA has great potential in estimating the flow direction of COW arteries using a dedicated post-processing method.

INTRODUCTION

Cerebral collateral circulation plays a pivotal role in maintaining cerebral blood flow, especially when principal conduits fail, and extending the treatment window prior to revascularization¹. The Circle of Willis (COW), which is the primary collateral circulation mechanism in the brain, bridges the interhemispheric blood flow pathways and between the anterior and posterior circulations, and can provide rapid response to cerebral blood flow alteration in acute vascular events². Therefore, a comprehensive evaluation of the structure and blood flow of COW is important for the diagnosis and treatment of cerebrovascular diseases.

To date, due to the wide availability of angiography techniques, such as digital subtraction angiography (DSA)³, computed tomography angiography (CTA)⁴, magnetic resonance angiography (MRA)⁵, the patency and caliber of the arterial segments in COW have been extensively explored regarding their characteristics and clinical relevance⁶. However, the blood hemodynamics within these segments were less studied and assessed in clinical practice, which could be largely attributed to the difficulty in its measurement. In general, the blood hemodynamics could be assessed either by monitoring the traveling of contrast agents within the vascular networks with time-resolved or artery-selective angiography techniques⁷, or by directly measuring the local blood flow velocity using techniques such as transcranial Doppler (TCD)⁸ and phase contrast (PC) MRI⁹. DSA is usable for evaluating the hemodynamics of COW but is limited by its invasiveness. Time-resolved CTA and contrast-enhanced MRA have difficulty in offering sufficient spatial-temporal resolution to depict the small-sized COW arteries¹⁰. While TCD provides flow direction information, visualization of the intracranial arteries is not infrequently limited by the lack of acoustic windows. PC MRI allows measurements of pixel-wise velocity for COW⁹ but suffers from long scan time and difficulty in choosing an appropriate encoding velocity to achieve good vessel visibility and accurate flow quantification for both large and small-sized arteries.

Non-contrast enhanced dynamic magnetic resonance angiography (dMRA) based arterial spin labeling (ASL) is an emerging technique that can achieve both high spatial resolution (e.g. 0.8 mm isotropic) and temporal resolution (up to ~100 ms) for 4D vascular imaging^{11–13}. It thus has great potential in characterizing the hemodynamics of intracranial arteries. Shao et al show that ASL dMRA can be used to quantify the arterial blood flow, arterial blood volume, arterial transit time, and mean transit time for application in arteriovenous malformation¹⁴. However, the usefulness of ASL dMRA for depicting flow in COW is yet to be explored.

Flow direction is an important feature of COW that is helpful in identifying the vessels responsible for ischemia, the brain regions potentially in a vulnerable state and needing special attention¹⁵. In this proof-of-concept study, we hypothesized that flow direction information within the COW can be derived from ASL dMRA. To test the hypothesis, we developed an ASL dMRA image analysis method to derive this information, and then evaluated its performance on a cohort with atherosclerotic diseases by using the velocity direction derived from 3D PC MRI as the reference.

MATERIALS AND METHODS

Participants

The Institutional Review Board approved this study and all participants gave written informed consent prior to recruitment. As a sub-cohort of the study named Carotid Intraplaque Hemorrhage: MRI of Therapeutic Response and Clinical Sequelae, 52 subjects with the following inclusion criteria were recruited: age ≥ 18 ; no contradictions to MRI; asymptomatic from carotid disease; at least one carotid artery had $>15\%$ stenosis. The exclusion criteria of the study were as follows: subjects with systemic inflammatory disease or atrial fibrillation; pregnant; history of bilateral carotid endarterectomy or stenting; history of neck radiation therapy; severe chronic illness or chronic disability that will limit life span and may lead to incomplete study procedures.

MRI protocol

All MRI studies were conducted on a 3.0-T Philips Ingenia CX scanner (Philips, Best, the Netherlands) with a 32-channel array head coil. MRI protocol included 3D PC-MRI and a recently developed ASL dMRA technique, named iSNAP¹¹. iSNAP is a time-efficient multi-contrast cerebrovascular imaging sequence that can yield ASL dMRA, static MRA, vessel wall images, and T1W brain structural images simultaneously in a single scan. It consists of flow-sensitive alternating inversion recovery (FAIR) ASL preparations and 3D golden angle radial spoiled gradient echo readout. To obtain ASL dMRA from the iSNAP sequence, multiple images at different delays after the ASL preparation were reconstructed from subsets of the original 3D k-space data, by using the k-space weighted image contrast (KWIC) view-sharing reconstruction algorithm, and then subtraction of the images were performed between the ASL Control and Label acquisitions. Imaging parameters of the ASL dMRA with iSNAP were: turbo field echo factor 280, total number of turbo field echo shots 186, field of view $205 \times 180 \times 144 \text{ mm}^3$, voxel size $0.8 \times 0.8 \times 0.8 \text{ mm}^3$, TR/TE 7.6/2.7 ms, flip angle 6 degrees, total scan time 6.5 min. The ASL dMRA was reconstructed with 20 frames with a temporal resolution of 100ms (2s in total). Imaging parameters of 3D PC-MRI were: spoiled gradient recalled echo, field of view $180 \times 180 \times 70 \text{ mm}^3$, voxel size $0.5 \times 0.5 \times 1.0 \text{ mm}^3$, TR/TE 13/6 ms, flip angle 12 degrees, receiver bandwidth 96 Hz/pixel, VENC value 100 cm/s in all three directions, acquisition time 5 min.

Tracing of COW artery centerlines

Maximum intensity projection along the temporal dimension (tMIP) was generated from the ASL dMRA (Figure 1A), and then used to trace 3D centerlines of intracranial arteries, including that of COW, with a custom-made semi-automated intracranial artery feature extraction software named (iCafe)¹⁶. A typical artery centerline extraction example is shown in Figure 1B. The traced arteries included left and right internal carotid arteries at their carotid terminus (ICA), left and right anterior cerebral arteries at their A1 segments, anterior communicating artery (AComm), left and right posterior cerebral arteries at their P1 segments, left and right posterior communicating arteries (PComm), as shown in Figure 1C. Rigid registration was applied between the magnitude image from 3D PC and T1-weighted-like image obtained from iSNAP using SPM12 (<https://www.fil.ion.ucl.ac.uk/spm>). Then, the artery centerlines obtained from the ASL dMRA were translated to the co-registered 3D velocity map obtained from 3D PC-MRI.

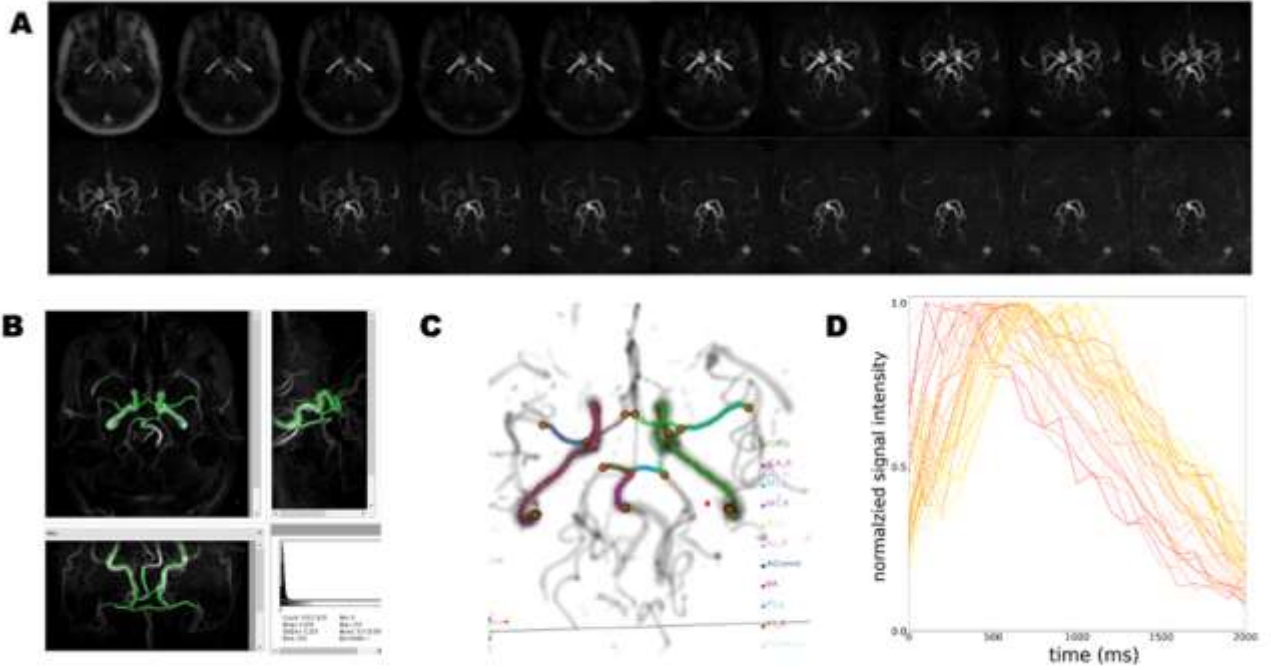


FIG 1. A) Representative ASL dMRA images obtained by the iSNAP sequence. B) Centerline tracing results based on the temporal maximum intensity projection (tMIP) of dMRA. C) The labeled COW arteries for flow direction estimation. D) Time signals along the centerline of ICA artery, measured from ASL dMRA. The red ones correspond to the proximal sites of ICA, while the light yellow ones correspond to the distal sites.

Flow direction analysis on 3D PC-MRI

Then, for each arterial segment, 3 cross-sectional images that are perpendicular to the artery centerline, as obtained from tMIP of ASL dMRA, at the 1/6, 3/6, and 5/6 of the segment, were generated. Vessel lumen contours were subsequently automatically extracted using the active contour method on the cross-sectional angiography images¹⁷, and manually corrected. Then, the flow direction in each vessel segment was determined by the average velocity vector of the 3 cross-sectional slices.

Flow direction analysis on iSNAP dMRA

Figure 1D shows the typical intensity time-curves extracted from the ASL dMRA for the voxels along the centerline of artery. The flow direction within the COW can be predicted by estimating the time-curve shift and identifying the source of the signal profile that reaches the peak earlier. It is worth noting that unlike cardiac-triggered 4D CTA or 4D flow MRI, the flow direction obtained from ASL dMRA is averaged across cardiac phases. Three principal methodologies, namely graph modeling¹⁸, bootstrap strategy¹⁹, and ensemble learning²⁰, were utilized to determine the time-curve shift from ASL dMRA. A graph model was constructed based on the COW's anatomy. The bootstrap strategy, a resampling approach in statistics and machine learning, can be used to estimate signal patterns from high-dimensional data. Ensemble learning, another technique from statistics and machine learning, combines multiple models to enhance predictive performance. The following is an in-depth explanation of each methodology.

An undirected graph with node features x_v and edges v were first built based on the morphology of the COW, as shown in Figure 2. Node features x_v represent a point on the centerline of the arterial segment with N time points, with A as the symbol of the adjacency matrix, and D as the symbol of the degree matrix. Each element of A represents whether there is a connection between two nodes v_i and v_j . D is a diagonal matrix, where each diagonal element D_{ii} stands for the number of nodes connected to node i . Laplace matrix L of the graph was derived by

$$L = D^{-\frac{1}{2}} A D^{-\frac{1}{2}}$$

By utilizing the low-pass characteristic of L , we can get a smoother graph X' after we multiply L to the node feature matrix X . Here smoother means features between adjacent nodes become more alike.

Next, the flow direction was determined using the filtered node feature matrix X' through the combination of bootstrap strategy and ensemble learning. For each arterial segment, four ensembled strategies were employed to calculate the flow direction independently. These strategies focused on the correlation between different parts of the targeted arterial segment and were subsequently combined to produce the final flow direction result, as shown in Figure 3. The targeted artery was divided into halves, with each half connected to the adjacent artery (which may be absent). The flow direction in the 'half target' segment was determined for the first two strategies, as illustrated in Figure 3B and 3C. Specifically, k pixels were randomly sampled at each time in each segment and repeated N times. The correlation between the points in each sampling from adjacent arterial segments, 'half target', and the 'other half target' segment was then calculated. The two correlation coefficients calculated in each sampling were compared, and the flow direction was assigned '+1' for the

antegrade direction and '-1' for the retrograde direction. Finally, the results were summed up, and the flow direction was saved for the final ensemble decision. For the third strategy (S3), half of the points in the target artery were randomly sampled each time and repeated N times. The correlation between distance and time-to-peak (TTP) was calculated. The flow direction was assigned '+1' for antegrade flow direction and '-1' for retrograde flow direction. The sum of the length N sequence was computed. The fourth strategy (S4) was similar to the first two, but the correlation was calculated between the adjacent arterial segment and the target artery instead of dividing into halves. If one side of the target artery was missing, the correlation on that side was considered equal to -inf. The final flow direction of the target artery was determined by whether the total sum of all four length N sequences was greater than zero.

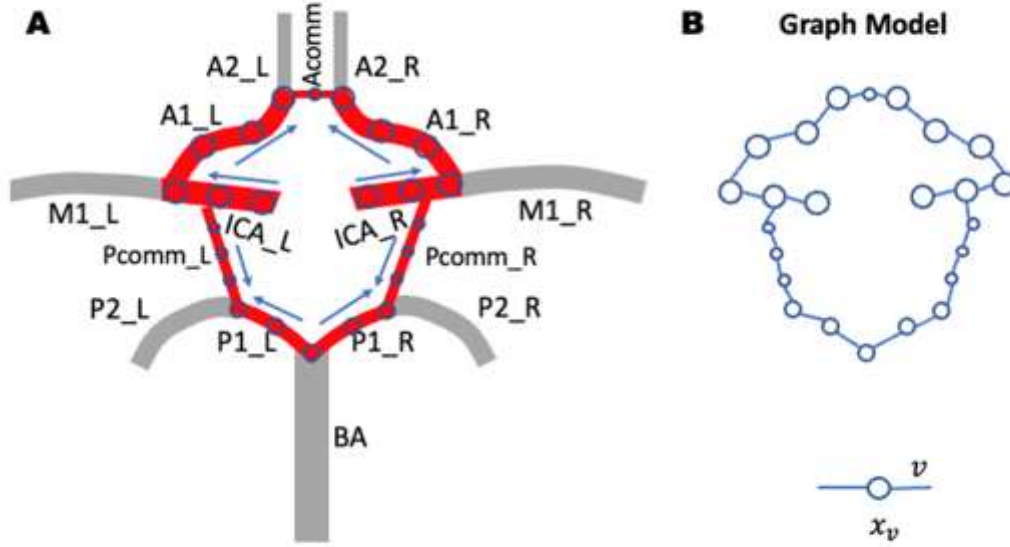


FIG 2. A) Predefined antegrade blood flow direction in the COW. B) The graph model built based on the COW.

Image quality control and data exclusion

On ASL dMRA, if the arterial centerline could not be clearly identified and traced by one experienced radiologist (>5years) and one experienced medical imaging analysis reviewer (>3years), the corresponding artery segment would be excluded from the analysis. On 3D PC, the artery segment would be excluded from the analysis if the lumen contours on all three cross-sectional slices could not be depicted by an automated 2D lumen contour segmentation algorithm from SPM12 (<https://www.fil.ion.ucl.ac.uk/spm>) and double checked by an experienced radiologist (>5years).

Ablation study

Ablation studies were performed to explore the individual and combined effects of the sampling time and number of sampling points on the estimation of flow direction, which will be evaluated by accuracy, sensitivity, and specificity. The sampling time ranges from 1000 to 5000, with an interval of 500. The number of sampling points ranges from 3 to 6, with an interval of 1. The number of sampling points should be at least 3, as this is the minimum number required to calculate the correlation coefficient. The accuracy, sensitivity, and specificity of the flow direction estimation were calculated for each setting.

Evaluation metrics and statistical analysis

Blood flow direction was defined as antegrade or retrograde. The predefined antegrade flow direction for the COW arteries is illustrated in Figure 2A. For communicating arteries, the flow direction was not predefined for AComm and the predefined antegrade flow direction in PComm is the anterior circulation to posterior circulation. Any blood flow direction opposite to the direction shown in Figure 2A was considered retrograde. Segment-wise accuracy, sensitivity, and specificity of the flow direction prediction results acquired by the proposed method on ASL dMRA were calculated, by using the flow directions estimated from 3D PC-MRI as the gold standard.

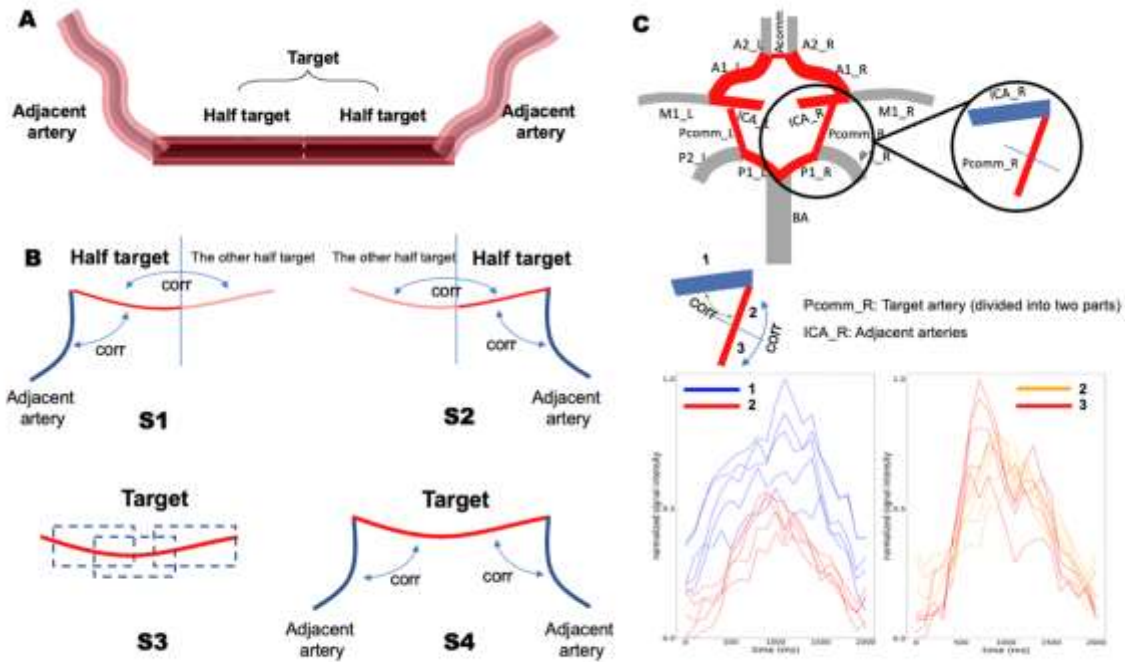


FIG 3. The 4 strategies employed in this study to estimate the flow direction of COW arteries based on ASL dMRA. A) Illustration of different parts of the target artery and its adjacent arteries. B) Schematics showing how the correlation coefficients were calculate flow direction. In these schematics, flow direction was estimated for the deep red segment, with the shallow red segment being the other half on the same artery and the deep blue segments being the adjacent arteries. C) An example showing how to derive flow direction for the target artery (right PComm) from strategy 1 in the COW. The correlation between the adjacent artery (right ICA, #1) and the first half of the target artery (#2) was first calculated, and then the correlation between the first half of the target artery (#2) and the other half of the target artery (#3) was calculated. The two plots only showed one sampling time with the number of sampling points equal to 5. Determination of the flow direction will depend on the sign of the sum of the correlation coefficient from part 1-2 and part 2-3.

RESULTS

Flow direction results from 3D PC-MRI

Among the 52 subjects, 340 arterial segments in COW were evaluated, including left and right ICA, left and right A1 and P1, AComm, left and right PComms. 6/340 (1.8%) artery segments were excluded due to low image quality of cross-sectional PC-MRI impeding assessment checked by an experienced radiologist (>5years). 23/340 (6.8%) segments are AComm. Among the rest of the segments, 281/340 (82.6%) had antegrade flow directions, while 30/340 (8.8%) had retrograde directions including left and right A1, P1, and PComm, according to the 3D PC-MRI.

Arterial segment summary and flow direction results from ASL dMRA

The length, and radius of the COW arteries measured from ASL dMRA as well as the accuracy of flow prediction is shown in Table 2. In 310/334 (92.8%) arterial segments, the flow directions obtained using ASL dMRA were consistent with those using 3D PC-MRI. The detailed prediction accuracy for each arterial segment is also shown in Table 2. Table 3, without including the AComm, shows the accuracy, sensitivity, and specificity of flow direction predictions from ASL dMRA with different analysis strategies. The final accuracy, sensitivity, and specificity after combining all strategies were 92.80%, 83.33%, and 93.96%, respectively. Among the 23 AComm arterial segments, 18/23 (78.3%) arterial segment flow directions were aligned with 3D PC-MRI, while 5/23 (21.7%) had wrong predictions.

Ablation study

The results of the ablation study are shown in Fig. 4. The optimal parameter combinations were a sampling time of 3000 and a number of sampling points of 3.

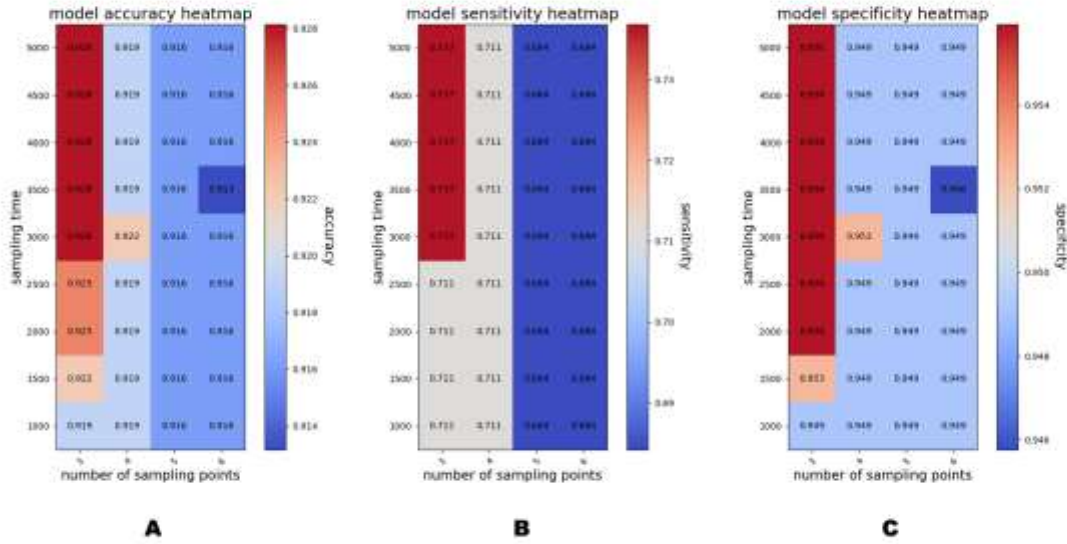


FIG 4. Accuracy (A), sensitivity (B), and specificity (C) of the flow direction estimation in the ablation study, in which different sampling time and the number of sampling points were used.

DISCUSSION

In the current study, we demonstrate the feasibility of using ASL dMRA to evaluate the flow direction in individual arterial segments of the circle of Willis by using a graph-based bootstrap technique. Using 3D PC-MRI as the reference, the proposed method can predict the flow direction with high accuracy, sensitivity, and specificity.

Method evaluation

The basic idea used in this study is to estimate the temporal shift of the signal curve from points on the arteries of the COW. The following methods were employed to improve the estimation. First, the arterial network of COW was represented as a graph. Such representation not only improves the characterization of the inherent connection between the arteries, but also serves as a low pass filter to reduce the noise in the time signal. Similar ideas were widely used in cognition studies to represent connections of neurons or in diffusion MRI models to describe functional interactions in brain structure^{21,22}. Secondly, the bootstrap strategy, a powerful statistical procedure to estimate target variables, was used to lower the variance and uncertainty of the prediction result. Thirdly, four different strategies were employed and combined to derive the final flow direction. This ‘ensemble learning’ strategy has been shown to improve the predictive performance²⁰. Specifically, in this study, the first two strategies focused on the flow pattern in two adjacent arterial segments, the third strategy focused on the flow direction within the arterial segment, and the last strategy focused on the completeness of the circle.

Most of the arteries with an inconsistent flow direction between 3D PC and ASL dMRA are the communicating arteries. This may be attributed to their small length and lower blood flow, which not only result in a larger noise but also make artery tracing more difficult. The fact that the flow directions inside the communicating arteries may vary over time²³, may also contribute to the discrepancy.

Significance and comparison to other modalities

The clinical significance of the COW is largely dependent on its role in redistributing the blood flow between the different flow territories and protecting the brain tissue against potential flow deficiency caused by cerebrovascular diseases. Therefore, assessing the COW’s flow condition is more important and desirable than only assessing its morphology, although the two aspects are somehow related. Retrograde flow, as assessed by the proposed method, is a critical aspect of flow dynamics. Previous studies have indicated that retrograde flow is often a sign of compromised hemodynamics, which can lead to several adverse outcomes such as increased risk of ischemic events and poor tissue perfusion^{24,25}. Additionally, Li et al. have discussed how retrograde flow can serve as a critical marker for assessing the severity of artery occlusions, significantly impacting clinical decision-making and prognostication²⁶. However, due to the limit of imaging techniques, many previous studies that explored the clinical relevance of the flow condition in COW only considered its morphological configuration²⁷. Therefore, developing a reliable imaging technique with good clinical acceptance and availability is important for facilitating the study and diagnosis of flow condition in COW.

Conventional DSA is recognized as the gold standard for assessing COW, attributed to its superior spatiotemporal resolution and vessel selectivity²⁸. However, its application has been limited by the invasiveness, ionizing radiation, and higher cost as compared to the imaging modalities. Another occasionally used technique is 4D-CTA, however, current 4D-CTA techniques have limited temporal resolution to acquire an accurate flow profile in collateral circulation²⁹. Although one previous study demonstrated their ability to acquire flow direction

and flow velocity using gamma distribution extrapolation³⁰, further validation work on 4D-CTA is still needed. 4D-flow MRI is another novel quantitative state-of-the-art technique to measure cerebral blood flow profile, however, more efficient reconstruction and post-processing methods are needed to solve the long scan time, low spatial resolution, and long processing times³¹. TCD ultrasound is a real-time, noninvasive, and cost-effective technique for evaluating collateral circulation by providing spectral flow waveforms, flow direction, and velocity information⁸. However, visualization of the intracranial arteries may be poor due to limited acoustic windows. There are several advantages for ASL dMRA including its non-invasive, non-radioactive nature, its high spatial and temporal resolution, facilitating accurate assessment of COW blood flow. Above all, ASL dMRA demonstrated accurate quantification results compared to PC-MRI.

Clinical applications

ASL dMRA has several potential clinical applications. Visualization of flow patterns could be helpful in the evaluation of collateral circulation for treatment planning when considering surgical arterial sacrifice³², revascularization surgeries in Moyamoya disease⁴, aneurysm treatment planning³³, and assessment of cerebrovascular reserve in combination with carbon dioxide challenge³⁴. In addition, it can also be used for the assessment of collateral flow patterns in chronic arterial occlusions³⁵, or assessment of potential etiologies in cryptogenic stroke³⁶, to determine flow patterns and potential arterial sources for emboli. Furthermore, the application of our proposed method with and without vascular stimulus could potentially identify flow redistribution patterns and detect vascular steal in stenotic occlusive disease, which will be explored in future studies³⁷.

Carotid stenosis and retrograde flow

An additional analysis was performed using Chi-square test to compare the incidence of retrograde flow between the subjects with any large carotid stenosis (>50%) and the subjects without. A trend was observed that the group with large stenosis tended to exhibit a greater incidence of retrograde flow, but the difference was not statistically significant (45.5% vs. 23.5%, $P = 0.26$). Further research with a larger sample size is needed to confirm this observation.

Limitations

There are several limitations in this study. First, the gold standard for flow direction measurement, i.e. DSA, was not available for the studied subjects. Therefore, 3D PC MRI was used as the reference, considering that it has been well-validated for measuring the flow in COW³⁸. However, we retrospectively included two Moyamoya disease patients from a pilot study who underwent both preoperative ASL dMRA and DSA imaging to support our study. The flow direction predictions from ASL dMRA using the proposed method are consistent with the flow directions from DSA (Supplemental materials). Second, the centerline of AComm could not be extracted accurately for some subjects, due to a low signal intensity and short length. This may compromise the flow direction estimation from ASL dMRA and 3D PC-MRI. Another limitation is that the sample size is small and only subjects with carotid atherosclerosis were included. This has limited the generalizability of the findings. Therefore, in the future, the proposed method needs to be further validated for other cerebrovascular diseases, such as intracranial atherosclerosis, cerebral aneurysm, arteriovenous shunting etc.

CONCLUSIONS

This proof-of-concept study shows that high temporal-spatial resolution ASL dMRA combined with a dedicated post-processing method can be used to estimate the flow direction in the COW with high accuracy. Therefore, ASL dMRA has the potential to become a useful noninvasive tool for assessing the collateral flow of COW in cerebrovascular diseases.

ACKNOWLEDGMENTS

Table 1. Clinical characteristics of the enrolled subjects (N=52).

Variable	Mean \pm SD or N (%)
Age	72.3 \pm 7.6
Male	29 (56)
BMI	28.0 \pm 3.7
Hypertension	27 (47)
Systolic blood pressure	144.0 \pm 15.7
Diastolic blood pressure	79.3 \pm 10.4
Use of antihypertensive drug	36 (67)
Diabetes	9 (16)
Smoking	13 (45)

BMI: body mass index

Table 2. Length, radius, and correct prediction counts for arterial segments (N=52).

Arterial segment	Length (mm)	Radius (mm)	Accuracy (Correct #/Total #)
ICA_R	89.8 ± 16.9	2.7 ± 0.4	98.07% (51/52)
ICA_L	87.9 ± 15.2	2.8 ± 0.3	98.04% (50/51)
A1_R	18.3 ± 3.4	1.9 ± 0.3	95.65% (44/46)
A1_L	17.5 ± 2.3	1.9 ± 0.3	97.78% (44/45)
AComm	4.2 ± 1.8	1.8 ± 0.4	78.26% (18/23)
PComm_R	15.1 ± 3.2	1.8 ± 0.4	86.67% (13/15)
PComm_L	14.9 ± 4.1	1.9 ± 0.3	94.44% (17/18)
P1_R	11.7 ± 4.7	2.2 ± 0.4	88.10% (37/42)
P1_L	10.9 ± 4.3	2.2 ± 0.3	88.10% (37/42)

R: right; L left; ICA: internal carotid artery; AComm: anterior communicating artery; PComm: posterior communicating artery

Table 3. Accuracy, sensitivity, and specificity of the four strategies, along with overall performance metrics.

Strategy	Accuracy	Sensitivity	Specificity
s1	47.60%	80.56%	43.96%
	(159/334)	(29/36)	(131/298)
s2	60.48%	30.56%	68.79%
	(202/334)	(11/36)	(205/298)
s3	78.44%	61.11%	80.54%
	(262/334)	(22/36)	(240/298)
s4	56.29%	75.00%	55.37%
	(188/334)	(27/36)	(165/298)
Overall	92.80%	83.33%	93.96%
	(310/334)	(30/36)	(280/298)

REFERENCES

1. Liebeskind DS. Collateral circulation. *Stroke* 2003;34:2279–84.
2. Liebeskind DS. Collateral lessons from recent acute ischemic stroke trials. *Neurol Res* 2014;36:397–402.
3. Modic M, Weinstein M, Chilcote W, et al. Digital subtraction angiography of the intracranial vascular system: comparative study in 55 patients. *Am J Roentgenol* 1982;138:299–306.
4. Zhang J, Wang J, Geng D, et al. Whole-Brain CT Perfusion and CT Angiography Assessment of Moyamoya Disease before and after Surgical Revascularization: Preliminary Study with 256-Slice CT. *PLOS ONE* 2013;8:e57595.
5. Hirooka R, Ogasawara K, Inoue T, et al. Simple Assessment of Cerebral Hemodynamics Using Single-Slab 3D Time-of-Flight MR Angiography in Patients with Cervical Internal Carotid Artery Steno-Occlusive Diseases: Comparison with Quantitative Perfusion Single-Photon Emission CT. *Am J Neuroradiol* 2009;30:559–63.
6. Wijesinghe P, Steinbusch HWM, Shankar SK, et al. Circle of Willis abnormalities and their clinical importance in ageing brains: A cadaveric anatomical and pathological study. *J Chem Neuroanat* 2020;106:101772.
7. Rojas-Villabona A, Pizzini FB, Solbach T, et al. Are Dynamic Arterial Spin-Labeling MRA and Time-Resolved Contrast-Enhanced MRA Suited for Confirmation of Obliteration following Gamma Knife Radiosurgery of Brain Arteriovenous Malformations? *AJNR Am J Neuroradiol* 2021;42:671–8.
8. Guan J, Zhang S, Zhou Q, et al. Usefulness of Transcranial Doppler Ultrasound in Evaluating Cervical-Cranial Collateral Circulations. *Interv Neurol* 2013;2:8–18.
9. Khan MA, Liu J, Tarumi T, et al. Measurement of cerebral blood flow using phase contrast magnetic resonance imaging and duplex ultrasonography. *J Cereb Blood Flow Metab* 2017;37:541–9.
10. Xu Y, Fu Y, Kedziorek D, et al. A comparison of time-of-flight mr angiography, contrast-enhanced mr angiography and ct angiography to evaluate vessel area in a rabbit peripheral arterial disease model. *J Cardiovasc Magn Reson* 2011;13:P366.
11. Chen Z, Zhou Z, Qi H, et al. A novel sequence for simultaneous measurement of whole-brain static and dynamic MRA, intracranial vessel wall image, and T₁-weighted structural brain MRI. *Magn Reson Med* 2021;85:316–25.
12. Suzuki Y, Fujima N, van Osch MJP. Intracranial 3D and 4D MR Angiography Using Arterial Spin Labeling: Technical Considerations. *Magn Reson Med Sci* 2020;19:294–309.
13. Yan L, Wang S, Zhuo Y, et al. Unenhanced Dynamic MR Angiography: High Spatial and Temporal Resolution by Using True FISP-based Spin Tagging with Alternating Radiofrequency. *Radiology* 2010;256:270–9.
14. Shao X, Zhao Z, Russin J, et al. Quantification of intracranial arterial blood flow using non-contrast enhanced four-dimensional dynamic magnetic resonance angiography. *Magn Reson Med* 2019;82:449–59.
15. De Caro J, Ciacchiarelli A, Tessitore A, et al. Variants of the circle of Willis in ischemic stroke patients. *J Neurol* <https://doi.org/10.1007/s00415-021-10454-4>.
16. Chen L, Mossa-Basha M, Sun J, et al. Quantification of morphometry and intensity features of intracranial arteries from 3D TOF MRA using the intracranial artery feature extraction (iCafe): A reproducibility study. *Magn Reson Imaging* 2018;57.
17. Kass M, Witkin A, Terzopoulos D. Snakes: Active contour models. *Int J Comput Vis* 1988;1:321–31.
18. Adali T, Ortega A. Applications of Graph Theory [Scanning the Issue]. *Proc IEEE* 2018;106:784–6.
19. Fushiki T. Bootstrap prediction and Bayesian prediction under misspecified models. *Bernoulli* 2005;11:747–58.
20. Polikar R. Ensemble based systems in decision making. *IEEE Circuits Syst Mag* 2006;6:21–45.
21. Wang J, Zuo X, He Y. Graph-based network analysis of resting-state functional MRI. *Front Syst Neurosci* 2010;4.
22. Hejazi S, Karwowski W, Farahani FV, et al. Graph-Based Analysis of Brain Connectivity in Multiple Sclerosis Using Functional MRI: A Systematic Review. *Brain Sci* 2023;13:246.
23. Zhou W, Lu M, Li J, et al. Functional posterior communicating artery of patients with posterior circulation ischemia using phase contrast magnetic resonance angiography. *Exp Ther Med* 2019;17:337–43.
24. Ahn SH, d'Esterre CD, Qazi EM, et al. Occult Anterograde Flow Is an Under-Recognized but Crucial Predictor of Early Recanalization With Intravenous Tissue-Type Plasminogen Activator. *Stroke* 2015;46:968–75.
25. Yan S, Feng H, Ma L, et al. Predictors of successful endovascular recanalization in patients with symptomatic nonacute intracranial large artery occlusion. *BMC Neurol* 2023;23:376.
26. Li M, Zhang J, Pan J, et al. Obstructive coronary artery disease: reverse attenuation gradient sign at CT indicates distal retrograde flow--a useful sign for differentiating chronic total occlusion from subtotal occlusion. *Radiology* 2013;266:766–72.
27. Tan IYL, Demchuk AM, Hopyan J, et al. CT Angiography Clot Burden Score and Collateral Score: Correlation with Clinical and Radiologic Outcomes in Acute Middle Cerebral Artery Infarct. *Am J Neuroradiol* 2009;30:525–31.
28. Eaton RG, Shah VS, Dornbos D, et al. Demographic age-related variation in Circle of Willis completeness assessed by digital subtraction angiography. *Brain Circ* 2020;6:31–7.
29. Grunwald IQ, Kulikovski J, Reith W, et al. Collateral Automation for Triage in Stroke: Evaluating Automated Scoring of Collaterals in Acute Stroke on Computed Tomography Scans. *Cerebrovasc Dis Basel Switz* 2019;47:217–22.
30. Mizutani K, Arai N, Toda M, et al. A Novel Flow Dynamics Study of the Intracranial Veins Using Whole Brain Four-Dimensional Computed Tomography Angiography. *World Neurosurg* 2019;131:e176–85.
31. Dunås T, Holmgren M, Wåhlin A, et al. Accuracy of blood flow assessment in cerebral arteries with 4D flow MRI: Evaluation with three segmentation methods. *J Magn Reson Imaging* 2019;50:511–8.
32. Complete or Partial Parent Artery Sacrifice: Effect of Vessel-Occlusion Strategies on Complete Obliteration of Complex Aneurysms | Elsevier Enhanced Reader. <https://doi.org/10.1016/j.wneu.2020.12.050>.
33. de Rooij NK, Velthuis BK, Algra A, et al. Configuration of the circle of Willis, direction of flow, and shape of the aneurysm as risk factors for rupture of intracranial aneurysms. *J Neurol* 2009;256:45–50.
34. Liu P, De Vis J, Lu H. Cerebrovascular reactivity (CVR) MRI with CO₂ challenge: a technical review. *NeuroImage* 2019;187:104–15.
35. Werner GS, Ferrari M, Heinke S, et al. Angiographic assessment of collateral connections in comparison with invasively determined collateral function in chronic coronary occlusions. *Circulation* 2003;107:1972–7.
36. Markl M, Semaan E, Stromberg L, et al. Importance of variants in cerebrovascular anatomy for potential retrograde embolization in cryptogenic stroke. *Eur Radiol* 2017;27:4145–52.
37. Mandell DM, Han JS, Poublanc J, et al. Quantitative Measurement of Cerebrovascular Reactivity by Blood Oxygen Level-Dependent MR Imaging in Patients with Intracranial Stenosis: Preoperative Cerebrovascular Reactivity Predicts the Effect of Extracranial-Intracranial Bypass Surgery. *AJNR*

Am J Neuroradiol 2011;32:721–7.

38. Yamashita S, Isoda H, Hirano M, et al. Visualization of hemodynamics in intracranial arteries using time-resolved three-dimensional phase-contrast MRI. *J Magn Reson Imaging* 2007;25:473–8.

SUPPLEMENTAL FILES

Subjects

We retrospectively included Moyamoya disease (MMD) patients from a pilot study that was originally aimed to test the developed ASL dMRA imaging sequence. The pilot study included 9 MMD patients, but only 2 underwent both preoperative ASL dMRA and DSA imaging. Therefore, only the 2 cases (one male, 50 years; the other female, 39 years) were used for comparing ASL dMRA and DSA.

Imaging

DSA was performed within one week after the MRI. The ASL dMRA scan used the same imaging parameters as the one in the manuscript. Intra-arterial DSA was performed on a digital angiography unit (DFP-8000D; Toshiba Medical). Frontal and lateral view DSA images were acquired after injection of a 4–10 mL bolus of the iodinated contrast agent (Iopamiro; Bracco Sine Pharmaceutical) at 2–5 mL/s in the bilateral common carotid arteries and bilateral vertebral arteries.

Analysis of flow direction

The flow direction of circle of Willis (COW) arteries, including left and right internal carotid arteries at their carotid terminus (ICA), left and right anterior cerebral arteries at their A1 segments, anterior communicating artery (AComm), left and right posterior cerebral arteries at their P1 segments, left and right posterior communicating arteries (PComm), on the ASL dMRA was estimated using the proposed method in the manuscript. DSA images were reviewed, blinded to the patients' clinical information and the MRI data, by an experienced neuroradiologist (>20 years) and the flow direction of COW arteries was determined. Using DSA as the reference, the accuracy of flow direction estimation on ASL dMRA was calculated.

Analysis of flow direction

In both the two MMD patients, the left A1, right A1 and AComm, as well as left PComm and right PComm, could not be identified on ASL dMRA. For the remaining 10 COW arteries (left and right ICA, P1 and basilar artery), the flow direction obtained using ASL dMRA was all consistent with that using DSA. The DSA and ASL dMRA images of an MMD patient are shown below:

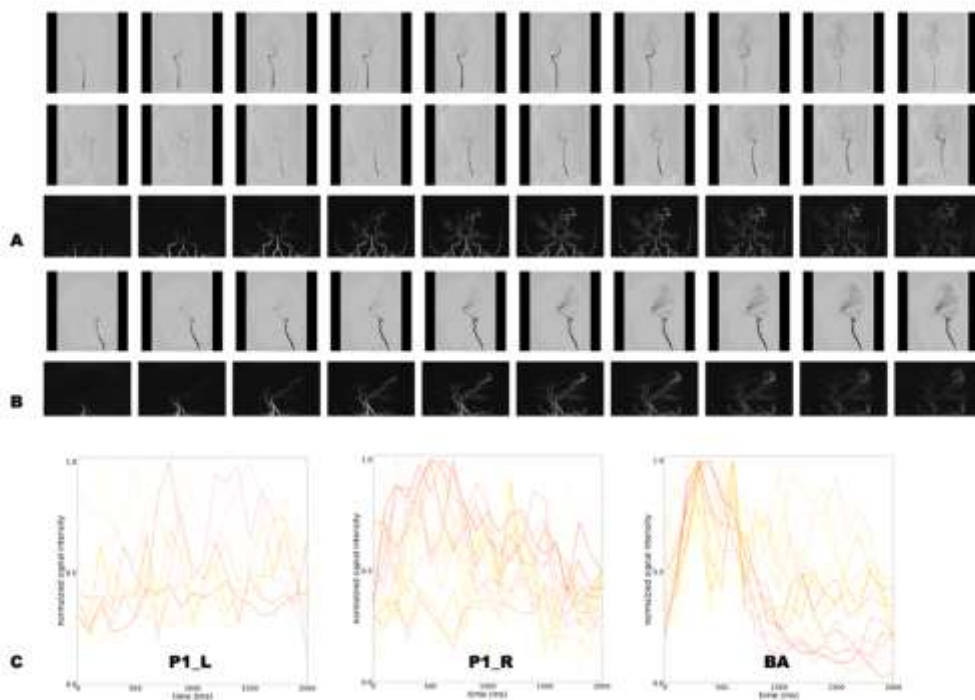


FIG S1. Comparative visualization of DSA and ASL dMRA image on an MMD patient. A) showcases a side-by-side comparison of 10 selected frames from DSA following injection into the left and right vertebral arteries, and 10 corresponding frames from dMRA. Both sets of frames are presented in the coronal view. B) features 10 selected frames from a sagittal view. C) showcases of the signal intensity curves for the left and right P1 segments from A) and signal intensity curves for basilar artery from B), illustrating the temporal changes in signal intensity captured by dMRA.